Preparation and Characterization of Cellulose-based Activated Carbon by Cesium Chloride Chemical Method

Conglin Zhang, Haichao Li,* and Bingxuan Du

Carbon adsorbent material with a specific surface area as high as 436 m^2/g was prepared by chemical activation method using cellulose as raw material and cesium chloride as activator, and its structure was characterized. Its adsorption performance on methylene blue solution was investigated, and the adsorption thermodynamics of crystalline violet dye at different temperatures was studied. The results showed that the surface of the prepared activated carbon material was smooth with abundant pores. The methylene blue adsorption value was as high as 176 mg/g, and it could adsorb methylene blue solution quickly and efficiently. It had good adsorption effect on crystal violet solution, the saturated adsorption amount reaches 281 mg/g at 40 °C, and the removal reached 92%, which indicated a self-heating adsorption reaction. Thus, CsCl could be used as an activator of wood raw material for the preparation of activated carbon samples.

DOI: 10.15376/biores.19.1.1295-1304

Keywords: Cellulose; Cesium Chloride; Activated carbon

*Contact information: Qinghai Nationalities University, Key Laboratory of Applied Physical Chemistry of Qinghai Province, Qinghai810007, China; *Corresponding author: lihaichao@vip.163.com*

INTRODUCTION

Lignocellulose is the most abundant natural raw material, with annual production exceeding 180 billion tons (Deng *et al*. 2023). Cellulose makes up 30 to 50 percent of it. It is an inexpensive, biodegradable, and renewable polymer that is fibrous and tough and insoluble in water. Vitamins and cellulose products are environmentally benign and can be returned to the carbon cycle through natural decomposition. Although cellulose has many applications and uses, one current use for large quantities of cellulose is as an adsorbent in various forms, such as raw cellulose, modified cellulose, or to prepare activated carbon (Zhang *et al*. 2022). The relatively low adsorption capacity of raw and modified cellulose and the widespread use of activated carbon have prompted researchers to explore the possibility of preparing activated carbon from sources such as cellulose and cellulosic materials.

Typical yields of carbon from lignocellulosic materials are 20 to 30 wt% during the carbonization step, and after the activation step, total yields are about 10 wt% (Li *et al*. 2020). The pore structure of the carbon is insufficient after the carbonization step, so an activation step is required. During the activation process, the spaces between the aromatic lamellae are filled with a variety of carbonaceous compounds and unorganized carbon that may have filled the interstices during the carbonization process. The carbonized material is converted into a form containing a large number of randomly distributed pores of various shapes and sizes, resulting in a product with an extended and very high surface area. The

carbonized material is further treated using chemical or physical activation to increase surface area and porosity (Bai *et al.* 2017; Fujishige *et al*. 2017).

Dassanayake *et al.* (2016) obtained activated carbon with a specific surface area of 750 m^2/g by carbonization and CO_2 activation of cellulose, having a total pore volume of 0.43 cm^3/g and a volume of micropores (pore width < 2 nm) of 0.27 cm^3/g, and adsorbing CO_2 up to 3.7 mmol/g and 5.8 mmol/g at 0 °C and 1 atm. Tuomikoski *et al.* (2019) activated lignocellulose at 800 °C using steam as a physical activator to obtain activated carbon with a specific surface area of 1080 m^2/g and a pore volume between 0.02 to 0.80 cm^3/g. The cellulose-based activated carbon obtained by Liu *et al.* (2021) had a high specific surface area of 477.14 m^2/g and a high oxygen content of 11.9%. It was applied to CE for a printable mesoscopic PSC (p-MPSC) of a hole-free conductor, which promotes the wettability and contact between CE and chalcogenide.

Cesium chloride is a precious salt lake resource. In this study, cesium chloride was used as an activator to activate cellulose by chemical activation method. The activation effect of cesium chloride on cellulose was explored, and microporous carbon adsorbent materials were prepared and their adsorption capacity for dyes was investigated.

EXPERIMENTAL

Materials

Cellulose (250 μm，$(C_6H_{10}O_5)_n$) and CsCl (AR, 99.9％) were purchased from Aladdin. The reagents were used directly without secondary treatment, and the experimental water was deionized water.

Preparation of Activated Carbons

Cellulose powder and CsCl were mixed in a crucible in the ratio of 5:1 and impregnated with 20 mL of deionized water. The purpose is for CsCl to be uniformly dispersed in the cellulose powder to give full play to the activation effect. The crucible was placed in an oven at 70 °C until completely dried. After drying, the crucible was taken out, and the crucible was put into a muffle furnace. The temperature was increased to 700 °C at a rate of 10 °C/min, and the product was obtained by holding the activation at 700 °C for 2 h. The product was washed repeatedly with deionized water until the pH value of the filtrate was close to neutral. Then the activated samples were filtered, dried, ground in the mortar and pestle and weighed to obtain the activated carbon. The cellulose-based activated carbon made at 700 °C is abbreviated as AC700.

Characterization Methods

Methylene blue adsorption was determined with reference to GB/T12496.10-2015 test method for wood-based activated carbon. The specimen was mixed with a certain amount (in milliliters) of methylene blue solution and filtered. The absorbance of the filtrate was measured spectrophotometrically. The concentration was lower than that of the standard solution at the specified concentration, and the number of milliliters of methylene blue required is the methylene blue adsorption value of the activated carbon specimen (Jia *et al.* 2017).

N_2 adsorption and desorption were carried out at 77k by a surface area and pore structure instrument (miniX, McMurray Tic Ltd.). (Weng *et al.* 2023)

A field emission scanning electron microscope (FESEM) model SU8010 from Hitachi, Japan was used to observe the microstructural features of activated carbon. An appropriate amount of activated carbon was taken and adhered to a specimen sheet of double-sided adhesive, and then sprayed with gold in a vacuum coater with an intensifying voltage of 20 kV, an acquisition of 100 s, and a scanning spacing of 15 mm (Nasrullah *et al.* 2017).

XRD testing was performed using Rigaku smartlab (Japan). The diffraction angle range 2θ=10 to 80° and the diffraction rate 4 °/min. The final diffraction spectrum obtained was used to characterize the activated carbon and to determine its microcrystalline structure (Nilmoung *et al.* 2020). XPS detection using Thermo Scientific Escalab 250Xi+, USA. X-ray photoelectron spectroscopy (XPS) was performed on a Thermo Scientific ESCALab 250Xi+ using 150W monochromated Al Kα (1,486.6 eV) radiation. A 500 µm X-ray spot was used for XPS analysis. The base pressure in the analysis chamber was about 3×10^{-10}mbar. Typically, the hydrocarbon C1s line at 284.8 eV from adventitious carbon is used for energy referencing (Zhang *et al.* 2020).

FTIR detection was performed using a Thermo Fisher NICOLET IS5. Infrared spectra were obtained by scanning in the wavelength range of 4000 to 400 cm^{-1}, and the functional groups of the activated carbon materials were analyzed by infrared spectroscopy (Nasrullah *et al.* 2017)

A Thermo Fisher DxR was used for roman assay. The graphitization degree of activated carbon was analyzed at an excitation wavelength of 532 nm. Raman analysis is an effective method to analyze the microstructure of charcoal materials, and its results are complementary to those of XRD (Jiang *et al.* 2022).

All test methods were carried out three times for each condition.

Thermodynamics

Three 0.1 g/L activated carbon samples were weighed and placed in 250 mL conical flasks, and the adsorption temperatures were set at 20, 30, or 40 °C. The adsorption was carried out by shaking under a water-bath shaker with a rotational speed of 180 r/min for 20 min, and 100 mg/L crystal violet solution was added dropwise. Samples were centrifuged, and the adsorption and removal rates were calculated by taking an appropriate amount of the supernatant and measuring its absorbance.

Thermodynamic parameters play an important role in the adsorption process. They can predict the spontaneity of adsorption. The thermodynamic parameters of adsorption of adsorbent on the adsorbent surface were determined based on the experimental data at 20 ℃ (293.15 K), 30 ℃ (303.15 K), and 40 ℃ (313.15 K), and the Gibbs equation and Van't Hoff equation were used to calculate the Gibbs' free energy (ΔG^0), enthalpy (ΔH^0) and entropy (ΔS^0), which are shown below. The equations are shown below,

$$lnK_d = -\frac{\Delta H^0}{RT} + \frac{\Delta S^0}{R'} \quad (1)$$

$$K_d = \frac{q_e}{c_e} \quad (2)$$

$$\Delta G^0 = -RTlnK_d \quad (3)$$

where R is the gas constant (8.314 J • mol^{-1} • K^{-1}), T is the adsorption temperature (K), K_d is the partition coefficient, q_e is the amount adsorbed at equilibrium (mg • g^{-1}), and c_e is the concentration of adsorbate at equilibrium (mg • L^{-1}).

RESULTS AND DISCUSSION

The samples from the five experiments were mixed into a single sample for characterization and experimental analysis.

Characterization of Activated Carbon

Specific surface area is an important parameter of activated carbon with pore size structure and an important factor affecting the adsorption performance of adsorbent. The adsorption and desorption curves and pore size distribution of activated carbon are shown in Fig. 1, and the specific surface area parameters at activation temperature are shown in Table 1.

Table 1. Characterization Results of Produced Activated Carbon Sample

Sample	Yield (%)	Specific Surface Area (m^2/g)	Pore Volume (cm^3/g)	Average Pore Size (nm)	Adsorption capacity of methylene blue (mg/g)
Cellulose carbon	7.42	436	0.22	1.99	176

As shown in Table 1, the activated carbon sample activated at 700 °C had a specific surface area of 436 m^2/g, a pore volume of 0.22 cm^3/g, and an average pore size of 1.99 nm, which showed that the activation of cellulose by CsCl at 700 °C yielded activated carbon materials with higher specific surface area and small pore sizes, most of which were microporous. According to the new IUPAC specification-2015 (Lee *et al.* 2016), the adsorption-desorption isotherm was of type I(b), as can be seen in Fig. 1(a)(b), and the adsorption isotherm had a larger slope in the low relative pressure region.

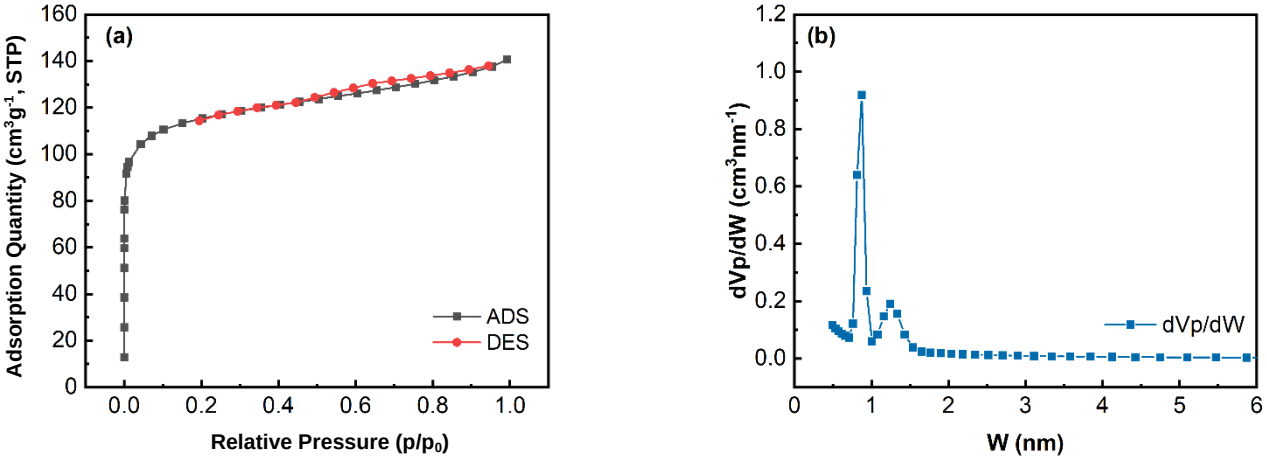

Fig. 1. (a) N_2 adsorption-desorption isotherms at 77 K, (b) Pore size distribution of activated carbon

The N_2 adsorption tends to equilibrate gradually with the increase of the relative pressure, which is mainly attributable to a strong interaction between the adsorbent and the adsorbate. The hysteresis loop almost coincided with the adsorption isotherm with a saturated adsorption platform, and the reaction pore size distribution was more uniform, indicating that the activated carbon was either a microporous material or a mesoporous

material close to microporous. The pore size distribution of the activated carbon material can be seen from Fig. 1(b), and the vast majority of the pore sizes were distributed at the 0.87 nm and 1.24 nm position, which shows that the activated carbon material had an extremely fine pore size and was a microporous material.

The surface morphology of the activated carbon was observed using a scanning electron microscope, and the results are shown in Fig. 2. The surface of the activated carbon was smooth and can be seen to have many fine pores. With the increase of temperature, the cellulose underwent carbonization and activation, forming pores of various shapes and sizes. This indicates that CsCl can enter the cellulose interior well during the activation process and leave the structure with developed voids. The activated carbon material has an adsorption ability and can adsorb dyes such as methylene blue.

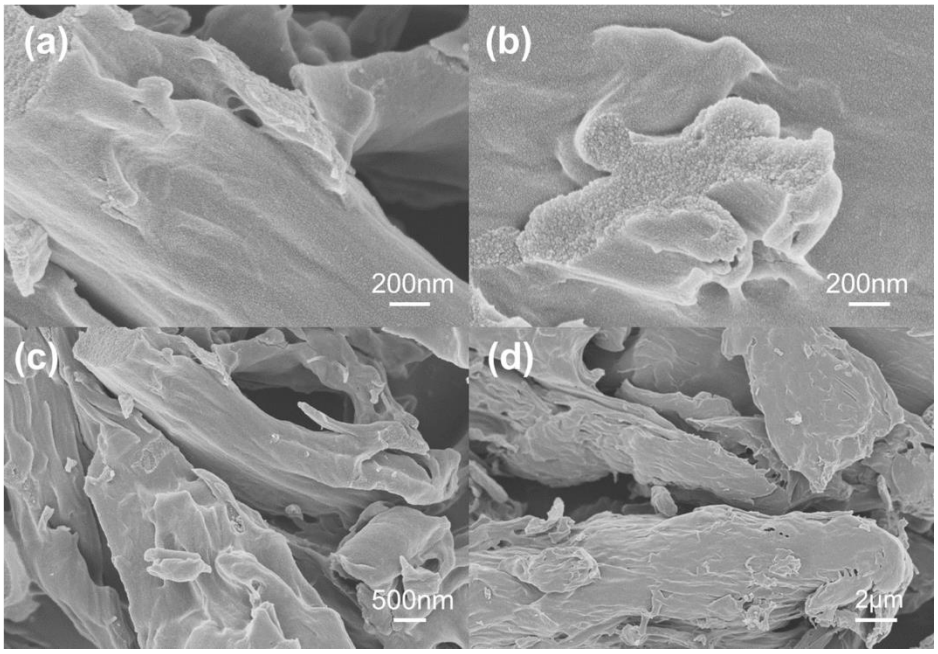

Fig. 2. SEM images of AC700 at 200 nm (a,b), 500nm (c) and 2 μm (d)

Figure 3 shows the Raman and XRD spectra of cellulose activated carbon, respectively. As shown in Fig. 3(a), the two distinct broad peaks at 1350 cm^{-1} and 1580 cm^{-1} are labeled as D and G bands, respectively. The D-band indicates defects, disorder and amorphous structure similar to graphite, and the G-band corresponds to the lattice vibrations of its graphitic character. In general, the graphitization of carbon increases gradually with increasing heat treatment temperature (Agarwal 2019). The I_D:I_G ratio of AC700 was 0.8491, indicating that the cellulosic activated carbon had a high degree of graphitization (Queiroz *et al.* 2021). The broad diffraction peaks of cellulose-based activated carbon at 2θ = 26° and 44° point to the (002) and (100) facets of graphene, respectively, with the (002) facet corresponding to standard graphite. The (100) corresponds to graphite layer diffraction (Wang *et al.* 2017), and the peaks at the (002) facet indicate that the cellulose-based activated carbon material had a high degree of graphitization. The (100) facet indicates the amorphous structure of the cellulose-based activated carbon material, which is in agreement with the XRD results.

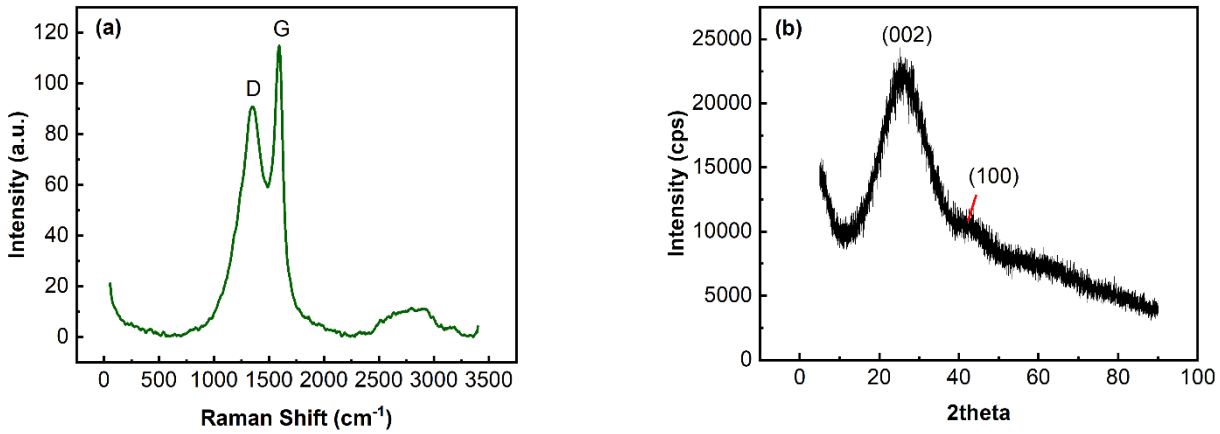

Fig. 3. (a) Raman spectrum of AC700, (b)XRD patterns of AC700

The AC700 FTIR plot is shown in Fig. 4(a). AC700 contains C-O, C=C, and O-H.

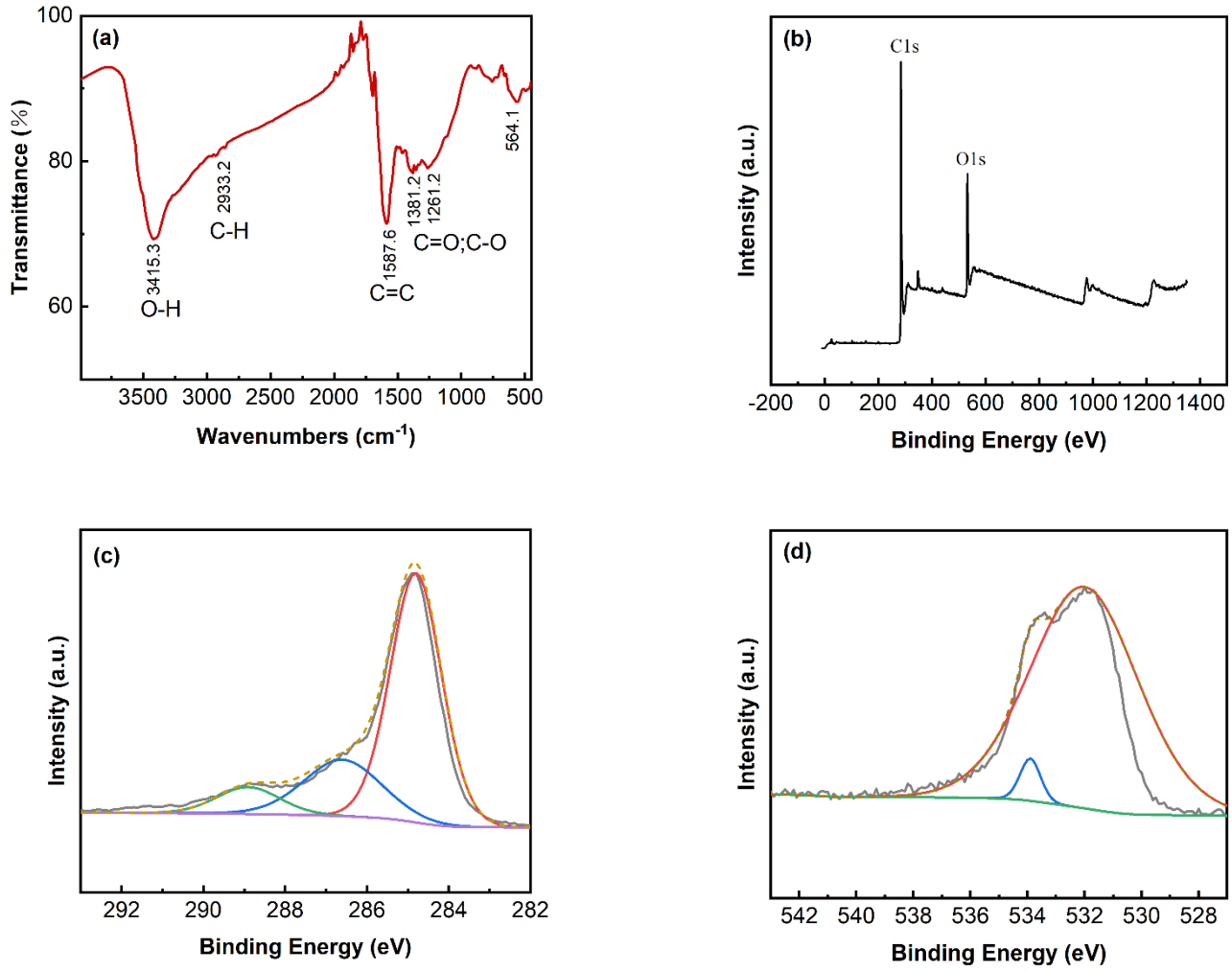

Fig. 4. (a) FTIR of AC700, XPS wide scan spectra (b) of AC700, C1s spectra (c), O1s spectra (d) of AC700

Previous studies have found that oxygen-containing functional groups affect the chemisorption capacity of activated carbon (Dittmann *et al.* 2022). As can be seen from Fig. 4(b)(c), subpeak fitting to C1s resulted in three peaks at 284.8, 286.7, and 289.1 eV, which correspond to C=C, C-O, and C=O bonds, respectively (Burg *et al.* 2002). The O1s partial peak fit has two peaks at 532.1 and 534.2 eV, corresponding to C=O and C-O, respectively (Quan *et al.* 2021), which support each other with the FTIR data.

Adsorption thermodynamics

The adsorption and removal rates of AC700 on crystalline violet solution are shown in Fig. 5. The adsorption of AC700 on the crystal violet solution was 239 mg/g at 20 °C, and the removal rate was 84%. At 30 °C, the adsorption amount was 261mg/g, and the removal rate was 88%. When the temperature was increased to 40 °C, the adsorption amount reached 281mg/g, and the removal rate was 92%. With the increase of temperature, the adsorption amount of AC700 on the crystalline violet solution was elevated with better removal effect.

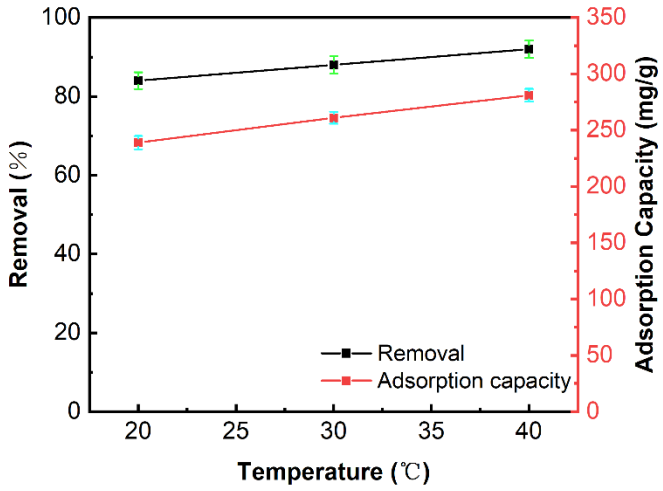

Fig. 5. Effect of adsorption temperature on adsorption properties of AC700

Calculated according to thermodynamic equations (1)(2)(3), the results of the thermodynamic study of adsorption of crystalline violet by AC700 are shown in Table 2 and, the van't Hoff relationship for adsorption of crystalline violet by AC700 is shown in Fig. 6.

Table 2. Thermodynamic Parameters Values for the Adsorption of Crystal Violet onto AC700

Temperature (°C)	Thermodynamics			
	$\ln K_d$	ΔG^θ (KJ·mol^{-1})	ΔH^θ (KJ·mol^{-1})	ΔS^θ (J·mol^{-1}·K^{-1})
20	2.704	-7.402	17.428	84.700
30	3.080	-8.249		
40	3.559	-9.129		

All the values of ΔG^θ were negative, indicating that the transfer of crystalline violet from solute to AC700 is a spontaneous process (Gupta and Singh 2018). In addition, ΔH^θ= 17.428 KJ·mol^{-1}, which is positive, indicates that the adsorption process is essentially a

heat-absorbing process and that higher temperatures are favorable for the adsorption process, following the physisorption mechanism. In addition, ΔS^{θ}=84.700 J·mol^{-1}·K^{-1}, which is positive, indicating that the degree of freedom gradually increases during the adsorption process.

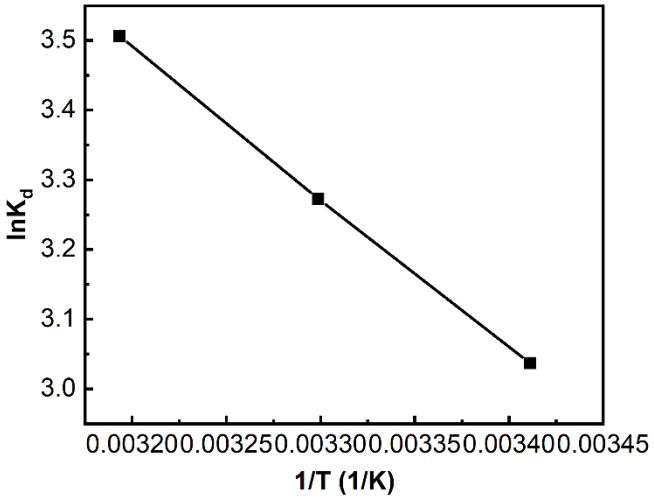

Fig. 6. Van't Hoff diagram of Adsorption of Crystal violet by AC700

CONCLUSIONS

1. Cellulose powder was activated by CsCl at 700 °C. The experimental results showed that CsCl had a beneficial activation effect on cellulose.
2. The activated carbon samples prepared at 700 °C reached a specific surface area of 436 m^2/g, a pore volume of 0.22 cm^3/g, an average pore size of 1.99 nm, and adsorbed 176 mg/g of methylene blue solution.
3. AC700 has a good adsorption effect on the crystal violet solution, the saturated adsorption amount reached 281 mg/g at 40 °C, and the removal rate reached 92%, which is a spontaneous heat absorption reaction.
4. It was demonstrated that CsCl can be used as an activator for the activation of wood raw materials for the preparation of activated carbon samples.

ACKNOWLEDGEMENTS

This work was supported by the Key R&D and Transformation Program of Qinghai (2022-QY-210).

REFERENCES CITED

Agarwal, U. P. (2019). "Analysis of cellulose and lignocellulose materials by Raman spectroscopy: A review of the current status," *Molecules* 24(9), article 1659. DOI: 10.3390/molecules24091659

Bai, Q., Xiong, Q., Li, C., Shen, Y., and Uyama, H. (2017). "Hierarchical porous cellulose/activated carbon composite monolith for efficient adsorption of dyes," *Cellulose* 24, 4275-4289. DOI: 10.1007/s10570-017-1410-y

Burg, P., Fydrych, P., Cagniant, D., Nanse, G., Bimer, J., and Jankowska, A. (2002). "The characterization of nitrogen-enriched activated carbons by IR, XPS and LSER methods," *Carbon* 40, 1521-1531. DOI: 10.1016/s0008-6223(02)00004-0

Dassanayake, R. S., Gunathilake, C., Jackson, T., Jaroniec, M., and Abidi, N. (2016). "Preparation and adsorption properties of aerocellulose-derived activated carbon monoliths," *Cellulose* 23, 1363-1374. DOI: 10.1007/s10570-016-0886-1

Deng, W., Feng, Y., Fu, J., Guo, H., Guo, Y., Han, B., Jiang, Z., Kong, L., Li, C., Liu, H., Nguyen, P., Ren, P., Wang, F., Wang, S., Wang, Y., Wang, Y., Wong, S. S., Yan, K., Yan, N., Yang, X., Zhang, Y., Zhang, Z., Zeng, X., and Zhou, H. (2023). "Catalytic conversion of lignocellulosic biomass into chemicals and fuels," *Green Energy & Environment* 8(1), 10-114. DOI: 10.1016/j.gee.2022.07.003

Dittmann, D., Saal, L., Zietzschmann, F., Mai, M., Altmann, K., Al-Sabbagh, D., Schumann, P., Ruhl, A. S., Jekel, M., and Braun, U. (2022). "Characterization of activated carbons for water treatment using TGA-FTIR for analysis of oxygen-containing functional groups," *Applied Water Science* 12, 1-13. DOI: 10.1007/s13201-022-01723-2

Fujishige, M., Yoshida, I., Toya, Y., Banba, Y., Oshida, K., Tanaka, Y., Dulyaseree, P., Wongwiriyapan, W., and Takeuchi, K. (2017). "Preparation of activated carbon from bamboo-cellulose fiber and its use for EDLC electrode material," *Journal of Environmental Chemical Engineering* 5, 1801-1808. DOI: 10.1016/j.jece.2017.03.011

Gupta, H., and Singh, S. (2018). "Kinetics and thermodynamics of phenanthrene adsorption from water on orange rind activated carbon," *Environmental Technology & Innovation* 10, 208-214. DOI: 10.1016/j.eti.2018.03.001

Jia, P., Tan, H., Liu, K., and Gao, W. (2017). "Adsorption behavior of methylene blue by bone char," *International Journal of Modern Physics B* 31, 16-19, article 1744099. DOI: 10.1142/s0217979217440994

Jiang, C. C., Li, X. C., Fan, J. A., Fu, J. Y., Nan, X., Fu, H., Li, J. J., Zheng, J. F., Zhou, X. S., and Wang, Y. H. (2022). "Electrochemically activated carbon–halogen bond cleavage and C–C coupling monitored by in situ shell-isolated nanoparticle-enhanced Raman spectroscopy," *Analyst* 147, 1341-1347. DOI: 10.1039/d2an00054g

Lee, S., Lee, M. E., Song, M. Y., Cho, S.Y., Yun, Y. S., and Jin, H. (2016). "Morphologies and surface properties of cellulose-based activated carbon nanoplates," *Carbon Letters* 20, 32-38. DOI: 10.5714/cl.2016.20.032

Li, S., Lin, Z., He, G., and Huang, J. (2020). "Cellulose substance derived nanofibrous activated carbon as a sulfur host for lithium-sulfur batteries," *Colloids and Surfaces A: Physicochemical and Engineering Aspects* 602, article 125129. DOI: 10.1016/j.colsurfa.2020.125129

Liu, C., Gao, C., Wang, W., Wang, X., Wang, Y., Hu, W., Rong, Y., Hu, Y., Guo, L., Mei, A., and Han, H. (2021). "Cellulose-based oxygen-rich activated carbon for printable mesoscopic perovskite solar cells," *Solar RRL* 5, article 2100333. DOI:

10.1002/solr.202100333
Nasrullah, A., Bhat, A. H., Naeem, A., Isa, M. H., and Danish, M. (2017). "High surface area mesoporous activated carbon-alginate beads for efficient removal of methylene blue," *International Journal of Biological Macromolecules* 107, 1792-1799. DOI: 10.1016/j.ijbiomac.2017.10.045
Nilmoung, S., Khajonrit, J., Sonsupap, S., and Maensiri, S. (2020). "Activated carbon nanofibers/aluminium doped-copper manganese ferrite composite nanostructures for electrochemical capacitors," *Journal of Energy Storage* 31, article 101777. DOI: 10.1016/j.est.2020.101777
Quan, C., Wang, H., Jia, X., and Gao, N. (2021). "Effect of carbonization temperature on CO2 adsorption behavior of activated coal char," *Journal of the Energy Institute* 97, 92-99. DOI: 10.1016/j.joei.2021.04.003
Queiroz, A. L. P., Kerins, B. M., Yadav, J., Farag, F., Faisal, W., Crowley, M. E., Lawrence, S. E., Moynihan, H. A., Healy, A., Vucen, S., and Crean, A. M. (2021). "Investigating microcrystalline cellulose crystallinity using Raman spectroscopy," *Cellulose* 28, 8971-8985. DOI: 10.1007/s10570-021-04093-1
Tuomikoski, S., Kupila, R., Romar, H., Bergna, D., Kangas, T., Runtti, H., and Lassi, U. (2019). "Zinc adsorption by activated carbon prepared from lignocellulosic waste biomass," *Applied Sciences* 9(21), 4583. DOI: 10.3390/app9214583
Wang, J., Liu, T., Huang, Q., Ma, Z., Chi, Y., and Yan, J. (2017). "Production and characterization of high quality activated carbon from oily sludge," *Fuel Processing Technology* 162, 13-19. DOI: 10.1016/j.fuproc.2017.03.017
Weng, X., Wang, Z., Zhang, B., Yu, X., Liu, X., and He, T. (2023). "Polyimide and polystyrene-based activated carbon nanofibers with tubular structure for supercapacitor," *Polymers for Advanced Technologies* 34, 1990-2000. DOI: 10.1002/pat.6026
Zhang, H., Xing, L., Liang, H., Ren, J., Ding, W., Wang, Q., Geng, Z., and Xu, C. (2022). "Efficient removal of Remazol Brilliant Blue R from water by a cellulose-based activated carbon," *International Journal of Biological Macromolecules* 207, 254-262. DOI: 10.1016/j.ijbiomac.2022.02.174
Zhang, Q., Zhu, J., Yan, Q., Sun, M., Yang, S., and Zhao, P. (2020). "The high electrochemical performance of N-doped active carbon with the shape of nanospheres in 1-ethyl-3-methylimidazolium tetrafluoroborate," *Ionics* 26, 5037-5043. DOI: 10.1007/s11581-020-03624-3

Article submitted: November 8, 2023; Peer review completed: December 16, 2023; Revised version received and accepted: January 1, 2024; Published: January 8, 2024.
DOI: 10.15376/biores.19.1.1295-1304